FACILITY UPGRADES FOR THE HIGH HARMONIC ECHO PROGRAM AT SLAC'S NLCTA

B. Garcia*, M.P. Dunning, C. Hast, E. Hemsing, T.O. Raubenheimer
SLAC, Menlo Park, California, USA
D. Xiang, Shanghai Jiao Tong University, Shanghai

Abstract

The Echo program currently underway at SLAC's Next Linear Collider Test Accelerator (NLCTA) aims to use Echo-Enabled Harmonic Generation (EEHG) to produce considerable bunching in the electron beam at high harmonics of a 2400 nm seed laser. The production of such high harmonics in the EUV wavelength range necessitates an efficient radiator and associated light diagnostics to accurately characterize and tune the echo effect. We have installed and commissioned the Visible to Infrared SASE Amplifier (VISA) undulator, a strong focusing two meter long planar undulator of Halbach array design with 1.8 cm period length. To characterize the output radiation, we have designed, built, and calibrated a grazing incidence EUV spectrometer which operates between 12–120 nm with resolution sufficient to resolve individual harmonics. An absolute wavelength calibration is achieved by using both EEHG and High Gain Harmonic Generation (HGHG) signals from the undulator.

INTRODUCTION

The NLCTA at SLAC is a low-energy X-band test accelerator which delivers a beam at up to 165 MeV with normalized projected emittance of <2 mm-mrad, and bunch charge of up to 200 pC. The current layout of the main NLCTA beamline is shown in Figure 1 (for a discussion of the previous state of the facility and upgrades, see [1]), and we briefly review it here. The beam is generated from a UV photocathode illuminated by a 266 nm, 1 ps long laser pulse and accelerated through a 1.6 cell BNL/SLAC/UCLA S-band gun. After, it is boosted to 60 MeV by an X-band accelerating structure (X1), and continues to the Echo portion of the beamline where it is accelerated again to 120 MeV (X2). An orbital bump is generated by small chicane (C0) to allow insertion of the first seed laser, which modulates the beam in the first undulator (U1), followed by the first dispersive chicane (C1), second modulator (U2), and final dispersive chicane (C2). An additional boost is provided by the third X-band structure (X3) to bring the beam energy to ~160 MeV, where the beam then enters the two meter VISA undulator (U3) to radiate. Finally, photons can be diverted into either the Extreme Ultraviolet (EUV) or Vacuum Ultraviolet (VUV) spectrometer and associated diagnostics, and electron beam energy is finally measured with a dipole energy spectrometer.

The NLCTA is currently involved in investigating advanced beam phase space manipulation techniques, particularly Echo-Enabled Harmonic Generation (EEHG) [2]. This technique involves using a two-modulator, two-chicane setup in order to generate density modulations in the electron beam at a high harmonic of the initial seed laser. The first laser modulator imprints an energy modulation on the beam, which is then macroscopically sheared by a strong first chicane. This creates a fine energy banding structure in the electron beam, effectively decreasing the slice energy spread of the individual beamlets. The beam is then modulated in a second undulator, and this modulation converted into density modulation by standing the energy modulation upright (similar to the manipulation in the more common High-Gain Harmonic Generation scheme [3]). Thus, a density modulation recoheres at a wavenumber given by $k = nk_1 + mk_2$, where n, m are integers, and k_1, k_2 are the wavenumbers of the first and second laser (which may be identical). This allows, for example, the single stage seeding of a x-ray free-electron laser via conventional lasers with harmonic numbers of perhaps up to 100 [4]. It is worth noting that such single stage seeding is difficult with alternate schemes, as the required energy modulation to reach high harmonics quickly exceeds the FEL bandwidth ρ, while in EEHG the required modulation remains comparatively small even for high harmonics.

At SLAC, this technique has been demonstrated in a series of proof of principle experiments, first to generate the 3rd and 4th harmonic of a 1600 nm seed [5]. This was then extended to the 15th harmonic of a 2400 nm seed, reaching down into the VUV at 160 nm [6]. One ultimate goal for the harmonic extension of the EEHG technique is to demonstrate the ~75th harmonic of a seed laser. At this harmonic, one can seed a x-ray FEL with a 266 nm laser and reach solidly into the x-ray regime, obtaining fully coherent light. Therefore, there has been a push to reach to these high harmonics at NLCTA, which has required the installation of a new radiating undulator along with an associated EUV photon spectrometer to characterize the harmonic generation.

THE VISA UNDULATOR

The previous radiation of the 15th harmonic of a 2400 nm seed laser was obtained using a 120 MeV beam and an X-band microwave undulator with tuneable K value and effective undulator period of 1.39 cm [7]. In order to more effectively radiate low wavelengths, we both increased the beam energy and installed a new, longer undulator.

To boost the beam energy, we added one additional X-band accelerating structure (X3) of 1 meter length following C2. This structure in the current configuration provides an additional 45 MeV of beam energy, bringing the total

* bryantg@stanford.edu

ISBN 978-3-95450-134-2

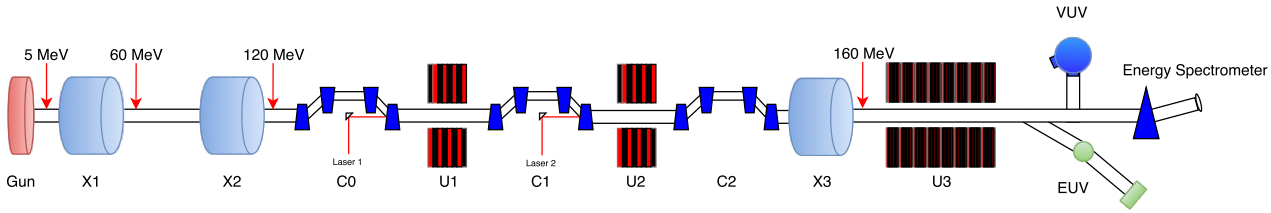

Figure 1: Layout of the NLCTA Echo beamline

energy entering the radiating section to 165 MeV. Furthermore, this acceleration occurs following the EEHG phase space modulation. Experimentally, we see that the EEHG bunching survives this final acceleration section. This observation hints at the possibility of performing complicated phase space manipulations at low beam energy, thus allowing lower powered lasers, and only later boosting to a final beam energy.

The installation of X3 and facility limitations in RF power necessitated a permanent magnet undulator. For this purpose, a two meter long planar undulator, known as the Visible to Infrared SASE Amplifier (VISA) was installed [8]. The VISA was originally designed as a test undulator for LCLS to reach saturation within a short distance by means of a high FEL paramater ρ and short period length. As such, the VISA is a permanent magnet array of Halbach array design and has a period length of 1.8 cm, undulator parameter $K = 1.26$, and is equipped with a strong focusing array to minimize the beta function during radiation. The focusing is achieved by a FODO array with 24.7 cm period, resulting in an average matched beta function of about 50–100 cm for an 160 MeV beam.

The VISA undulator is equipped with four Optical Transition Radiation (OTR) screens which allow viewing of the beam and radiation at positions along the undulator. To aid in steering, the VISA has also been equipped with four "window frame" corrector magnets, which each provide up to a 2×10^{-3} rad kick independently in each the x and y direction. The individual VISA magnets were first aligned using the pulsed-wire setup, providing an accuracy near 50 µm for the magnetic axis [9]. Once on the beamline, the VISA was then aligned by means of a small guide laser injected into the beam pipe by means of a pop-in screen. The currently installed VISA in place on the NLCTA beamline is shown in Figure 2.

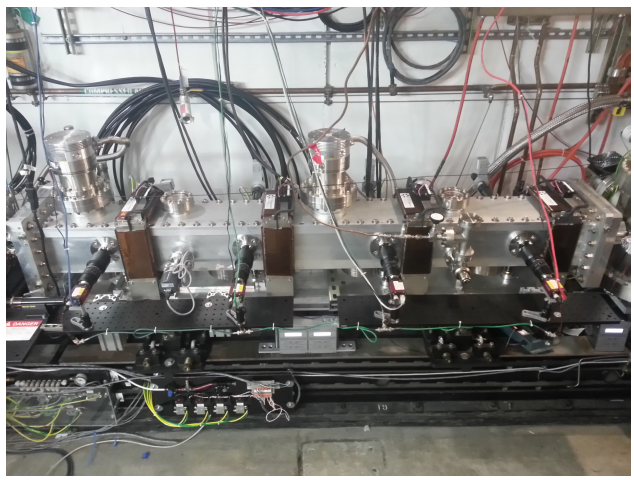

Figure 2: The VISA undulator in place on the NLCTA beamline. Visible are the four corrector magnets and pop-in observation screens.

THE EUV SPECTROMETER

In order to investigate the high harmonic radiation of the 2400 nm seed laser, we required additional diagnostics beyond those used in previous echo studies. In particular, the previous spectrometer was the commercially available McPherson model 234/302 scanning monochromator, equipped with a 2400 G/mm or 1200 G/mm corrected concave grating. Originally, this spectrometer was equipped with an Andor CCD camera and the efficiency of the setup was observed to drop precipitously below ~150 nm. Therefore, we constructed a custom grazing incidence EUV spectrometer to measure the light in the wavelength range 12–120 nm. The full assembly of the custom EUV spectrometer is shown in Figure 3. The light is first ejected from the beam path by means of a gold mirror at 15° angle of incidence

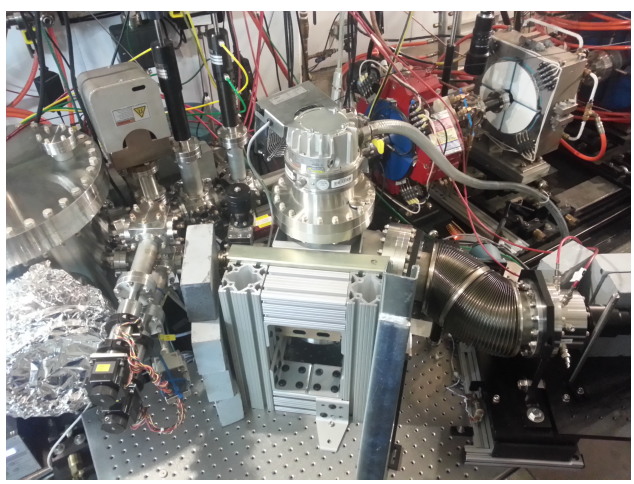

Figure 3: The custom EUV spectrometer. Light is ejected from the main beamline in the large chamber at the left, and passes through the double cube slit assembly. The chamber containing the grating is in the center, and the exit bellows is shown near the maximal shear position.

ISBN 978-3-95450-134-2

into the spectrometer arm of the assembly with a reflectivity of 60-80% over wavelengths of interest. During the design, several commercial slit solutions were considered but ultimately rejected due to limited available space, the need for high vacuum, and the desire to have a wide aperture range. We constructed a custom slit assembly using two small vacuum cubes with attached stepper motors to allow two parallel blades to close or open as a slit. A computer drawing of the slit assembly is shown in Figure 4. This setup also provides independent motion of each blade, allowing for translation of the combined slit while maintaining the aperture. Furthermore, the vertical design of the slit creates a minimal beamline footprint, allowing a relatively compact spectrometer assembly. The light then strikes a Hitachi 001-0639 (001-0640) aberration-corrected concave grating at an angle of 4.7°, corresponding to either the high or low energy configuration. These gratings have 600 (1200) G/mm, and a 3.7° blaze angle, focus to a flat field 469 mm from their center. These gratings allow reasonable focusing and efficiency in the range 22-124 (11-62) nm. This grating is mounted in a fixed configuration in a custom high-vacuum chamber.

Upon leaving the grating chamber, the light enters a large, 6" diameter bellows which is approximately 14" long. The diameter of the bellows was chosen to allow the dispersed light (including the zeroth order dispersion) to travel all the way to the focal plane without reflection. In order to capture the entire frequency spectrum from the grating, the end of the bellows is required to translate (parallel to the focal plane) approximately 120 mm. This large shear in the bellows structure necessitates a highly corrugated bellows, and the buckling of the individual bellows welds ultimately limits the spectrometer's upper wavelength range. The translation of the free bellows end is accomplished via a linear motion stage with a readback which is ultimately converted into a visible wavelength range.

The bellows end is then attached to a 40 mm MicroChannel Plate (MCP) detector (Model BOS-40, Beam Imaging Solutions). The MCP has a dual chevron configuration, CsI coating, 5 µm pore size, and gives a gain of approximately 10^4 when operated with a 2 kV high voltage power supply. The CsI coating provides relatively high detection efficiency from 10-150 nm, covering the whole range of interest for the Echo program. Behind the MCP is a P-43 phosphor screen, powered by a 5 kV power supply, which is then directly imaged with a camera.

Finally, the McPherson VUV spectrometer was moved to a separate portion of the beamline and equipped with a similar MCP detector (BOS-18, Beam Imaging Solutions). The gain of the MCP has allowed use of the McPherson spectrometer as a diagnostic tool down to ~50 nm.

CALIBRATION

Due to the flat field focusing of the EUV grating, the dispersion along the MCP is not constant, and varies depending on linear position (or equivalently, central wavelength). From the grating equation and the flat focus criterion, it is easy to see that

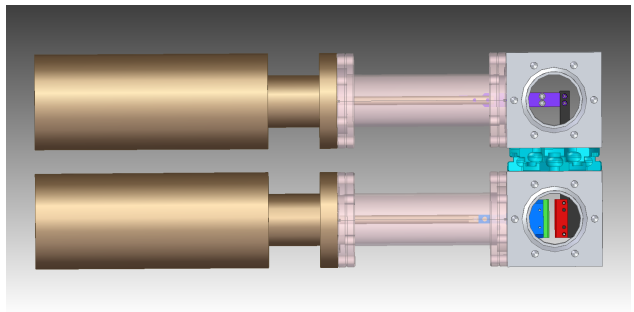

Figure 4: The custom slit assembly, showing the two blades on independent stepper motors.

$$x = r_{\text{focal}} \left(\frac{\sqrt{1 - (n\lambda - \sin\alpha)^2}}{n\lambda - \sin\alpha} \right)$$

Where x is the linear distance along the focal plane to the diffracted wavelength λ, n is the groove density, r_{focal} is the distance to the focal plane, and α is the angle of incidence.

In practice, the linear location of the zeroth order diffraction is first found and marked on the MCP screen as the reference zero pixel position. Then, displacements to desired wavelengths are calculated and the linear stage moved accordingly. The linear stage can be controlled to within a fraction of a mm, leading to a pointing accuracy in wavelength of $\lesssim$0.3 nm. Based on the central pointing wavelength and the known pixel position relative to the zeroth order, a wavelength scale can be established seamlessly over the entire range of spectral visibility.

In order to begin tuning of echo harmonics, attention is typically focused on the most easily attainable first. Therefore, typically the upgraded VUV spectrometer is first used to establish signals in the range 160-60 nm. From this configuration, using the low energy grating in the EUV spectrometer, the signal can be seamlessly tuned down into lower wavelength ranges.

Various misalignments and uncertainties can conspire to give theoretical uncertainties for wavelength pointing in the range of 1 nm. Therefore, it is desirable to have wavelength calibration guides to verify against. For this purpose, we use the radiated harmonics themselves to verify and calibrate the wavelength scale. As the laser wavelengths are highly stable and known, the corresponding echo harmonic positions are known to great accuracy. Although the beam energy may contain some significant jitter and chirp, the insensitivity of echo to this noise results in an incredibly reliable wavelength marker when echo signals are present [10]. Incidentally, this instability, present in the HGHG signal but not the EEHG, is often used to distinguish between the two when tuning for the echo effect. At high harmonic number, however, nearby harmonics may be nearly indistinguishable, leading to an ambiguity on the order of ~1 nm. First, where this ambiguity exists, one can investigate all relevant possibilities

ISBN 978-3-95450-134-2

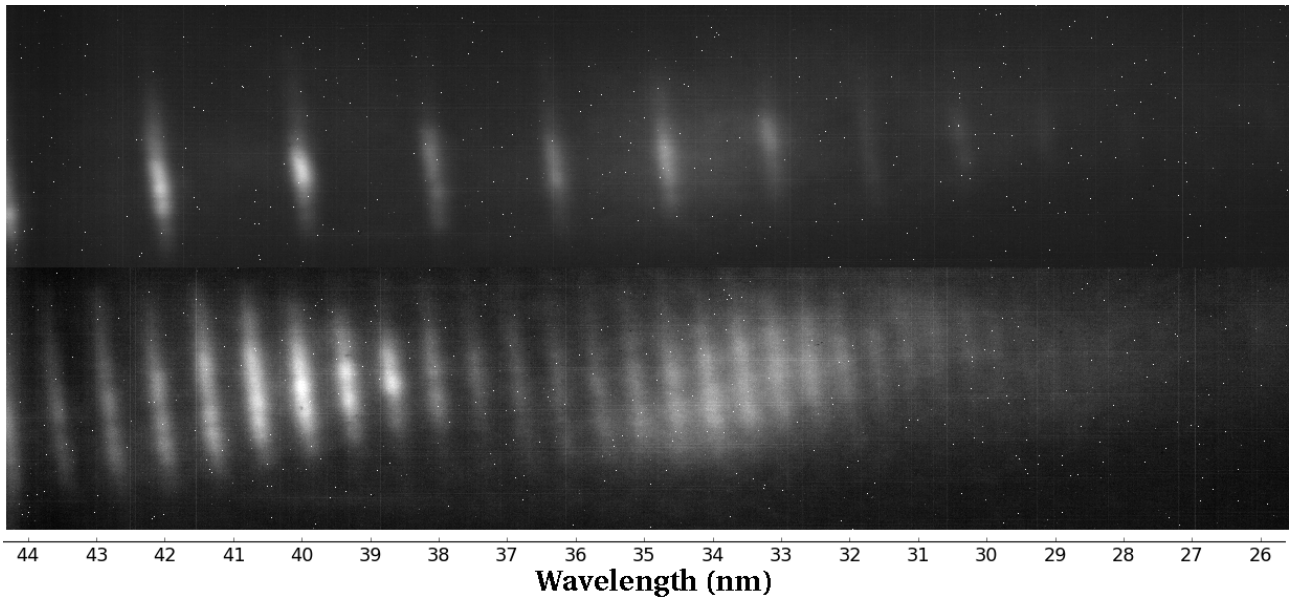

Figure 5: Calibration of the EUV spectrometer using images from the 800 nm (top) and 2400 nm (bottom) seed lasers. It is clear to identify the corresponding harmonic, providing a fine tune of the wavelength calibration as well as a check on the other methods described in this paper.

of harmonics and select the correct one via a χ^2 type analysis. To illustrate, select a particular harmonic and suppose it is the nth, knowing then that the nearby harmonics are the $n-1, n+1, n+2$ etc. The wavelength is known unambiguously enough to know the pixel dispersion $d(px)/d\lambda$, so that a set of calculated pixel positions for the various harmonics can be compared against their observed pixel positions. With this set of data, one can see which choice for n yields the lowest residual, and in practice there is always a clear choice.

To further strengthen the wavelength calibration of the device, the 800 nm laser was used to generate echo signals in the same region as the 2400 nm. Unfortunately, due to present constraints in the laser system, we are unable to quickly switch between the two, although with a stable beam the turnover time is low enough to cause only inconvenience. The 800 nm provides harmonics far enough apart to eliminate any ambiguity, and one can readily observe the overlap the nth harmonic from the 800 nm laser and the $3n$th from the 2400 nm laser as a final post in the wavelength calibration scale. This technique is demonstrated in Figure 5 where one can clearly identify 800 nm harmonics with their 2400 nm counterpart.

CONCLUSION

In order to investigate high harmonics of a 2400 nm seed laser, it was necessary to upgrade the beam energy, radiating undulator, and photon diagnostics at SLAC's NLCTA. To this end, the beam energy has been boosted by roughly 40 MeV by an additional accelerating structure (X3), a highly efficient strong focusing two meter VISA undulator was installed, and a custom EUV spectrometer for photon diagnostics in the range 12–120 nm was designed, installed, and calibrated.

These upgrades should enable the generation and radiation of laser harmonics up roughly through the 75th. Below this point, the VISA undulator will be radiating on its 6th harmonic, and it may prove difficult to detect any photons from this low efficiency radiation. To increase harmonic number, one can either increase the beam energy by adding an additional accelerating structure or increase the laser wavelength further into the infrared. RF limitations currently cap the energy gain of the structure X3 to about 45 MeV, but the addition of a SLED line could roughly double this energy, providing a beam of about 210 MeV. This upgrade would move the fundamental undulator harmonic to below 100 nm, and in principle allow the radiation of laser harmonics up past 100. We see no other limitations in terms of the NLCTA facility, so this upgrade would provide an environment to test the fundamental limits, and ultimate breakdown, of the EEHG process.

REFERENCES

[1] M. Dunning, C. Adolphsen, T. S. Chu, E. Colby, S. Gilevich, C. Hast, K. Jobe, C. Limborg-Deprey, D. McCormick, B. McKee *et al.*, "Status and upgrade of nlcta for studies of advanced beam acceleration, dynamics and manipulations," in *Proceedings of the 2011 Particle Accelerator Conference*, New York, NY, USA, 2011. [Online]. Available: http://jacow.org

[2] G. Stupakov, "Using the beam-echo effect for generation of short-wavelength radiation," *Phys. Rev. Lett.*, vol. 102, p. 074801, Feb 2009. [Online]. Available: http://link.aps.org/doi/10.1103/PhysRevLett.102.074801

[3] L. H. Yu, "Generation of intense uv radiation by subharmonically seeded single-pass free-electron lasers," *Phys. Rev. A*, vol. 44, pp. 5178–5193, Oct 1991. [Online]. Available: http://link.aps.org/doi/10.1103/PhysRevA.44.5178

ISBN 978-3-95450-134-2

[4] D. Xiang and G. Stupakov, "Echo-enabled harmonic generation free electron laser," *Phys. Rev. ST Accel. Beams*, vol. 12, p. 030702, Mar 2009. [Online]. Available: http://link.aps.org/doi/10.1103/PhysRevSTAB.12.030702

[5] D. Xiang, E. Colby, M. Dunning, S. Gilevich, C. Hast, K. Jobe, D. McCormick, J. Nelson, T. O. Raubenheimer, K. Soong, G. Stupakov, Z. Szalata, D. Walz, S. Weathersby, M. Woodley, and P.-L. Pernet, "Demonstration of the echo-enabled harmonic generation technique for short-wavelength seeded free electron lasers," *Phys. Rev. Lett.*, vol. 105, p. 114801, Sep 2010. [Online]. Available: http://link.aps.org/doi/10.1103/PhysRevLett.105.114801

[6] E. Hemsing, M. Dunning, C. Hast, T. O. Raubenheimer, S. Weathersby, and D. Xiang, "Highly coherent vacuum ultraviolet radiation at the 15th harmonic with echo-enabled harmonic generation technique," *Phys. Rev. ST Accel. Beams*, vol. 17, p. 070702, Jul 2014. [Online]. Available: http://link.aps.org/doi/10.1103/PhysRevSTAB.17.070702

[7] S. Tantawi, M. Shumail, J. Neilson, G. Bowden, C. Chang, E. Hemsing, and M. Dunning, "Experimental demonstration of a tunable microwave undulator," *Phys. Rev. Lett.*, vol. 112, p. 164802, Apr 2014. [Online]. Available: http://link.aps.org/doi/10.1103/PhysRevLett.112.164802

[8] R. Carr, M. Cornacchia, P. Emma, H.-D. Nuhn, B. Poling, R. Ruland, E. Johnson, G. Rakowsky, J. Skaritka, S. Lidia, P. Duffy, M. Libkind, P. Frigola, A. Murokh, C. Pellegrini, J. Rosenzweig, and A. Tremaine, "Visible-infrared self-amplified spontaneous emission amplifier free electron laser undulator," *Phys. Rev. ST Accel. Beams*, vol. 4, p. 122402, Dec 2001. [Online]. Available: http://link.aps.org/doi/10.1103/PhysRevSTAB.4.122402

[9] R. Ruland, D. Arnett, G. Bowden, R. Carr, B. Dix, B. Fuss, C. LeCocq, Z. Wolf, J. Aspenleiter, G. Rakowski *et al.*, "Visa undulator fiducialization and alignment," in *Proceedings of the 6th International Workshop on Accelerator Alignment, ESRF*, 1999.

[10] Z. Huang, D. Ratner, G. Stupakov, and D. Xiang, "Effects of energy chirp on echo-enabled harmonic generation free-electron lasers," in *Proceedings of the 2009 FEL Conference*, Liverpool, UK, 2009.

ISBN 978-3-95450-134-2